ELSEVIER

Desalination 113 (1997) 95–103

DESALINATION

Water permeability in ultrafiltration and microfiltration: Viscous and electroviscous effects

Ingmar H. Huisman*, Benoît Dutré, Kenneth M. Persson, Gun Trägårdh

Food Engineering, Lund University, PO Box 124, 221 00 Lund, Sweden
Tel. +46 (46) 222-9820; Fax +46 (46) 222-4622; E-mail: ingmar.huisman@livstek.lth.se

Received 24 May 1997; accepted 2 July 1997

Abstract

The applicability of Darcy's law for explaining the water permeabilities of polymeric UF membranes and ceramic MF membranes was investigated at various temperatures, viscosities, salt concentrations, and transmembrane pressures. It was found that Darcy's law explains the permeabilities well if the viscosity is corrected for electroviscous effects, temperature, and solute concentration. For polymeric UF membranes the compaction of the membranes needs to be taken into account as well. Ceramic MF membranes do not seem compressible for TMPs up to 80 kPa. Increasing the salt concentration from 30 μM to 0.1 M resulted in increases in water fluxes of 2% to 8% both for MF and UF membranes. This apparent permeability increase was explained by electroviscous effects: increased salt concentrations lead to lower zeta-potentials and thinner double-layers, offering less resistance to water passage. From the apparent permeability change the zeta-potentials of the membranes at pH $\approx$ 7 were calculated. Realistic zeta-potential values were obtained. Water flux measurements at various salt concentrations are thus a simple method to study zeta-potentials of membranes. The resistance (R_m) of the UF membranes was independent of temperature in the range 4–20°C, but increased with increasing transmembrane pressure (TMP). The increase could be described by a power law $\Delta R_m \sim \mathrm{TMP}^{0.8}$, typical for porous solids. The resistance of the ceramic MF membrane was independent of temperature and independent of TMP.

Keywords: Darcy's law; Permeability; Electroviscosity; Ultrafiltration; Microfiltration

1. Introduction

The development of methods for characterization and fouling studies of membranes, such as electron microscopy, pore size measurements, cut-off measurements of macromolecules and particles, and particle/protein adsorption to the membranes has improved the current knowledge of membrane structure and membrane separation properties [1]. The membrane permeability (or its inverse: the membrane resistance) has been found

*Corresponding author.

PII 0011-9164(97)00118-5

to play an important role in membrane processes. High permeabilities give high fluxes and thus more economic processes, but high fluxes can also increase concentration polarization and fouling [2,3]. Research on membrane permeabilities is thus of considerable importance.

Although the membrane permeability is often assumed to be roughly constant, it is known to be affected by membrane age and history, filtration time and applied transmembrane pressure (TMP). The process temperature can also affect the permeability. Tarnawski and Jelen [4] found a non-linear permeability increase for a polymeric UF membrane in the temperature region 20–45 °C, even after compensating for the viscosity decrease. They attributed this increase partly to a thermal expansion of the membrane material.

Due to the complexity of membrane filtration, the separation is generally described phenomenologically. For a rigorous treatment of various types of flow in porous media, see Nield and Bejan [5]. Many authors have used descriptions based on Darcy's law [6]:

$$J = \frac{TMP}{\mu R_m} \tag{1}$$

where R_m is the membrane resistance (in m^{-1}) and μ the dynamic viscosity of the liquid.

The viscosity is explicitly present in Darcy's law. It increases with solute concentration and decreases with temperature. If the membrane is sensitive to temperature changes, this must be taken into account in the membrane resistance term in Darcy's law. A possible method for analyzing the influence of temperature on R_m would be to do two series of flux measurements: one in which the viscosity of the feed liquid is increased by adding viscosity increasing solutes and one in which the viscosity of the feed liquid is increased by lowering the temperature. The temperature effect can then be separated from the viscosity effect.

Closely related to the viscosity is a physical phenomenon referred to as the *electroviscous effect*. If an electrolyte solution is pressed through a capillary with charged surfaces, ions are moved away from their preferred positions in the electrolyte double layer, associated with the surface. This costs extra energy and can be described as an increase in the apparent viscosity: the electroviscous effect. Levine et al. [7] showed that the apparent viscosity in a cylindrical pore is given by Eq. (2):

$$\frac{\mu_a}{\mu_0} = \left(1 - \frac{8\beta \left(\frac{e\zeta}{kT} \right)^2 (1-G)F}{(\kappa r)^2} \right)^{-1} \tag{2}$$

where μ_a is the apparent viscosity, μ_0 is the bulk viscosity of the electrolyte solution, ζ is the zeta-potential of the capillary surface, r is the capillary radius, and κ is the Debye constant. $1/\kappa$ is the Debye length which is a measure of the double layer thickness. At 20 °C the magnitude of the Debye length is

$$1/\kappa = 0.3014/\sqrt{[\mathrm{NaCl}]}\ \text{nm for 1:1 electrolytes (e.g., NaCl)}$$
$$1/\kappa = 0.1745/\sqrt{[\mathrm{MgCl_2}]}\ \text{nm for 1:2 electrolyte (e.g., } \mathrm{MgCl_2}) \tag{3}$$

G is a correction function for the overlapping double layers and F a correction function for high zeta potentials; G and F can be determined from graphs given in [7]. β is a dimensionless parameter describing the properties of the electrolyte.

$$\beta = \frac{\varepsilon_r^2 \varepsilon_0^2 k^2 T^2 \kappa^2}{16\pi^2 \mu \lambda e^2} \tag{4}$$

A schematic plot of μ_a/μ_0 vs. κr is shown in Fig. 1. It is seen that μ_a/μ_0 increases with κr for

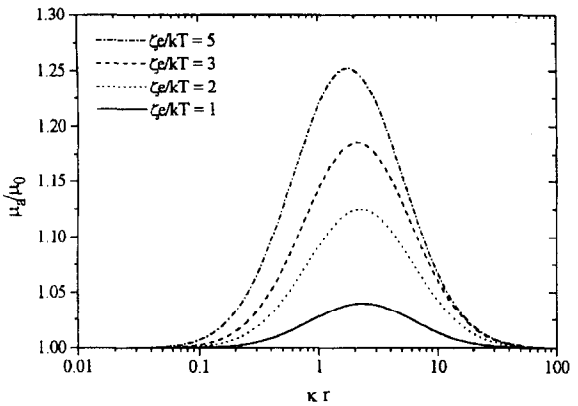

Fig. 1. Relative apparent viscosity vs. κr for various values of the zeta-potential. Redrawn schematically from [7].

κr less than about 2.5: increasing the salt concentration (i.e. increasing κ) gives a stronger electroviscous effect. μ_a/μ_0 reaches a maximum at $\kappa r \approx 2.5$ and then decreases for larger κr values: high salt concentrations lead to thinner double layers, which offer less resistance to water passage.

In membrane context it is often more convenient to use an apparent *permeability* ($1/R_{m,a}$) than an apparent viscosity. The apparent permeability is then defined as the permeability, obtained from Darcy's law if the bulk viscosity (μ_0) is used in stead of the apparent viscosity.

$$1/R_{m,a} \equiv \frac{\mu_0 J}{TMP} = \frac{\mu_0}{\mu_a}\ 1/R_m \qquad (5)$$

The electroviscous effect has been observed previously in membrane context. For both UF [8] and MF [9] fluxes have been reported to increase upon addition of salt to the feed solution. Heinemann et al. [9] found an apparent permeability improvement of 55% for a new MF membrane, which, however, cannot solely be explained by the electroviscous effect, which can cause an increase of about 25% as a maximum [7]. Moosemiller et al. [10] and Nazzal and Wiesmann [11] reported that the permeability of electrolyte solutions through alumina and titania membranes was greatest near the iso-electric point of these membranes, in accordance with electroviscous theory.

Porous media are very often sensitive to pressure. An easy empirical relation between hydraulic resistance and pressure is

$$R_m = R_{m,0} + k_c \cdot TMP^{\,n} \qquad (6)$$

where k_c is a constant and n is called the compressibility factor. For polymeric UF membranes it has been shown [4,12] that Eq. (6) describes observed resistances very well. The exponent n was found to be 0.8, and the factor $k \cdot TMP^n$ was about 25% of $R_{m,0}$ at a TMP of 4 bar. This effect was ascribed to compaction of the membrane.

Most authors use Darcy's law assuming a constant value for R_m and a constant value for the viscosity, often equal to the viscosity of water at 20°C. In the current paper it is investigated how well Darcy's law under these assumptions predicts actual water fluxes and what corrections are needed to obtain better predictions.

2. Materials and methods

2.1. Membranes

Three different polymeric flat-sheet UF membranes of the brand NADIR (Hoechst AG, Wiesbaden-Biebrich, Germany) were tested in a flat-sheet membrane module: polyaramid UF-PA-20 (NMWCO 20 kD), hydrophobic polysulfone UF-PS-100M (NMWCO 100 kD) and cellulose acetate UF-CA-100 (NMWCO 100 kD). Water permeabilities were also measured for a 20 kD NMWCO flat-sheet polysulfone DDS GR61 PP membrane and a 20 kD NMWCO flat-sheet cellulose acetate CA600 membrane, both from Dow Denmark Separation System (Nakskov, Denmark).

Polysulfone capillary X-Flow M3 UF membranes with a NMWCO of 80 kD were also

tested. They had an inside diameter of 1.35 mm and an outside diameter of 2.26 mm. The capillary module used was developed at our laboratory. It could handle one capillary membrane of 170 mm total length.

The ceramic MF membrane used was of the Membralox series produced by SCT (Bazet, France). The active layer of the membrane consisted of α-alumina. The membrane was tubular with an inner diameter of 6.85 mm and a pore size of 0.2 μm.

2.2. Solvents and chemicals

For the permeability experiments desalted water was used. The desalted water was produced from softened tap water which was desalted in an RO plant. It typically had a conductivity of 3 to 5 $\mu\Omega^{-1}cm^{-1}$ (corresponding to a NaCl concentration of $30 \cdot 10^{-6}$ M). All chemicals (sodium chloride, magnesium chloride, and glycerol) were of pro-analysis quality. For the viscosity measurements, desalted water was mixed with glycerol to final dynamic viscosities according to Table 1.

Table 1
Characteristics of the feed solutions. This table gives the glycerol concentrations that render the same viscosity effect at 20 °C, as do the shown temperature reductions

Viscosity (mPa·s)	Temperature of pure water (°C)	Equivalent glycerol content at 20 °C (% w/w)
1.002	20.0	0.00
1.120	15.6	5.00
1.284	10.6	9.625
1.486	5.7	14.75

2.3. Experimental equipment

For the flat-sheet UF membranes an automatic UF rig with temperature control, flux, pressure, and crossflow velocity measurement devices, and computerized permeate levelling was used. This rig, constructed at our laboratory, was described in detail elsewhere [13]. The accuracy of the temperature measurements was ±0.3 °C, for pressure ± 4 kPa, and for flux $\pm 0.5 \cdot 10^{-6}$ m/s (= 1.8 l/m² h).

For the capillary UF membranes a rig with a jacketed vessel (2 dm^3 capacity), temperature control, flux, and pressure measurement devices, and a back pressure valve was used. The temperature was controlled (±0.2 °C) by circulation of water from a thermostatic bath over the heat exchanger and the jacket of the vessel. The accuracy in flux measurements was ± 3% for TMPs higher than 20 kPa. For lower TMPs the fluxes were so low that the accuracy became poorer (±10%).

For the ceramic MF membrane a rig with temperature control, flux, pressure, and crossflow velocity measurement devices was used. A uniform transmembrane pressure (i.e., TMP independent of the position along the membrane) was guaranteed by a circulating flow on the permeate side, which created a pressure drop equal to the pressure drop on the feed side. More details of this rig, which was designed and constructed at our laboratory, are given elsewhere [14]. The accuracy of the temperature measurements was ±0.1 °C for pressure ± 500 Pa and for flux $\pm 0.5 \cdot 10^{-6}$ m/s (= 1.8 l/m² h).

2.4. Experiments

The flat sheet UF membranes were used mainly for studies on electroviscous effects. For each experiment a new membrane piece (28× 30 mm^2) was cut from a membrane sheet and mounted in the UF module. It was conditioned at 160 kPa TMP at 20 °C with desalted water for at least 30 min at a crossflow velocity of 10 m/s. The flux was then measured under the same conditions for at least 30 min or until the different flux measurements gave stable and reproducible values. For the electroviscosity measurements droplets of a 1 M salt solution of sodium chloride or magnesium chloride were added to increase the

salt concentration. The flux was measured for at least 30 min. More salt solution was added stepwise until no further flux increase could be achieved. Apparent permeabilities were calculated from these flux measurements using the uncorrected viscosity (0.001 Pa·s) and Darcy's law.

The capillary UF membranes were used mainly for studies on viscous effects and compaction. The piece of capillary membrane was first fixed into the module and then soaked in water for 24 h at room temperature. The permeate flux was measured for increasing and decreasing TMP. For each TMP value the permeate flux was measured as a function of time until a constant flux was reached. Each experiment was at least duplicated.

The ceramic MF membrane was used for studies on electroviscous effects, viscous effects and compaction. The same membrane was used for all experiments. For the electroviscosity measurements the TMP was set at 20 kPa and the resulting flux was measured at a crossflow velocity of 5 m/s. Sodium chloride salt was added stepwise to increase the salt concentration. Measured fluxes did not show any time dependence. For the compaction measurements the flux was measured as the TMP was increased stepwise.

3. Results and discussion

The permeability variation of the flat sheet UF membranes is presented in Table 2. For the NADIR membranes, the permeability standard deviation increases with increasing permeability. The DDS membrane GR61PP does not follow this trend; it has a rather low permeability but a high standard deviation. Large permeability standard deviations have been reported to be caused by the presence of a bimodal pore size distribution in the membrane [15].

The permeability increase caused by salt addition for different types of membranes is given in Table 3. Permeabilities for 0.1 M NaCl solutions were compared with desalted water. It is clear from these data that, both for cellulose acetate and for polysulfone, the 100 kD membranes show a larger electroviscous effect than the 20 kD membranes. The cellulose acetate membranes respond more than the polysulfone membranes. The α-alumina MF membrane responds more than the UF membranes. Since the zeta-potential of α-alumina membranes is known to be strongly dependent on pH [11,17], the obtained result might be only valid for the pH used here (≈7).

Table 2
Variation in pure water permeability for various membranes

Membrane	NMWCO (kd)	No. of observations	Permeability (10^{-14} m)
DDS GR61PP	20	11	20.1 ± 14.9
NADIR PA20	20	7	21.5 ± 1.3
NADIR CA100	100	10	45.8 ± 4.3
NADIR PS100M	100	20	77.2 ± 8.7

Table 3
Effect of 0.1 M NaCl instead of desalted water on permeability

Membrane	Assumed pore radius (nm)	Material	Relative permeability increase (%)
DDS GR61PP	9	Polysulfone	0.0
NADIR PS100M	15	Polysulfone	1.5
CA600	9	Cellulose acetate	3.8
NADIR CA100	15	Cellulose acetate	5.7
NADIR PA20	9	Polyaramid	5.1
SCT MF	100	α-alumina	8.0

The trend observed for cellulose acetate and polysulfone membranes (larger pore size gives larger electroviscous effect) is explained in Fig. 1. If the mean pore radii for 20 kD and 100 kD membranes are assumed to be 9 nm and 15 nm, respectively, it can be calculated that κr at $30 \cdot 10^{-6}$ M (salt concentration of desalted water) will have values of 0.16 and 0.27, respectively. It can easily be seen in Fig. 1 that for any zeta-potential μ_a is larger for $\kappa r = 0.27$ (100 kD membrane) than for $\kappa r = 0.16$ (20 kD membrane). The 100 kD membranes are thus expected to show larger apparent permeability increase, in accordance with observations.

Increasing the salt concentration under the assumption of a constant zeta-potential would according to Fig. 1 (and Fig. 6 in [7]) lead to an *increase* in apparent viscosity, and thus a *decrease* in apparent permeability. However, Fig. 2 shows clearly that an increase in salt concentration leads to an increase in apparent permeability. The only explanation for this phenomenon is that the zeta-potential decreases strongly with increasing salt concentration. In Fig. 1 it can be seen that a decrease in zeta-potential leads to a decrease in apparent viscosity.

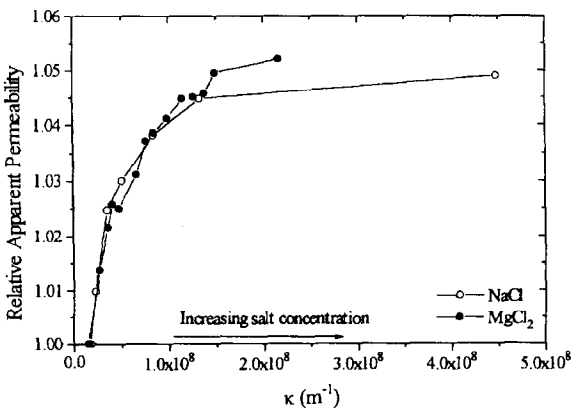

Fig. 2. Increase in relative apparent permeability upon salt addition for a NADIR CA100 membrane. Relative apparent permeability is the apparent permeability for a solution divided by the apparent permeability for desalted water.

The fact that the zeta-potential decreases with salt concentration is well known [16,17]. If it is assumed that a salt addition of 0.1 M reduces the zeta-potential so much that μ_a/μ reduces to 1, the zeta-potential at lower salt concentration can be calculated from the observed permeability differences.

Even though the electroviscous effects are presented here as an apparent permeability *increase* at increasing salt concentrations, it is physically more correct to describe the phenomenon as an apparent permeability *decrease* at low salt concentrations. The observed value for the apparent permeability ($\mu_0 \mu_a^{-1} R_m^{-1}$) is equal to the "real" permeability ($1/R_m$) at high salt concentrations. Decreasing the salt concentration increases both the zeta-potential and the double layer thickness, which causes μ_a to differ from μ_0 through electroviscous effects. This causes the apparent permeability to decrease below the "real" permeability. A consequence of this effect is that permeability values obtained with tapwater of high hygienic quality (salt concentration about $3 \cdot 10^{-3}$ M) can be more representative than permeability values obtained with desalted water, contrary to intuition. Experiments showed that tap water gave a higher apparent permeability than desalted water.

The MF membrane has a pore-size of 0.2 μm and thus a κr value of about 2.0 at a salt concentration of $30 \cdot 10^{-6}$ M. Increasing the salt concentration leads to larger values of κr, and it can be seen in Fig. 1 that this will lead to a decrease in μ_a, even if the zeta-potential would remain constant. A salt addition of 0.1 M increases κr to a value of about 100. It can be seen in Fig. 1 that, at $\kappa r = 100$, even for high zeta-potentials $\mu_a \approx \mu_0$. Therefore, zeta-potentials can be calculated from the permeability difference between the 0.1 M solution and other solutions.

Using the graphs given by Levine et al. [7] and assuming a mean pore size of 15 nm for the 100 kD and 9 nm for the 20 kD membranes, values for the UF membrane zeta-potentials were obtained. The zeta-potential for the polysulfone

membranes is about 62 mV, and for the cellulose acetate membranes about 88 mV. Zeta-potentials obtained by streaming potential measurements on polysulfone membranes have values of about 5 mV [18], and zeta-potentials obtained by electroosmosis measurements about 20 mV [19]. The authors of both publications mention that these values are underpredictions and that the real zeta-potential value is expected to be higher.

The exact value obtained for the zeta-potential from the electroviscosity data depends strongly on the assumed pore-size. An approximate permeability-based mean pore-size was used for the UF membranes [1,20]. Since the inaccuracy in pore size is so large, the obtained zeta-potentials have a low accuracy, certainly not better than ±50%.

The zeta-potential obtained for the α-alumina membrane at pH ≈ 7 is 28 mV, which is realistic if compared with zeta-potentials obtained from streaming potential measurements [21]. The accuracy in the pore size data of the ceramic MF membrane is much higher than that of the UF membranes. The obtained zeta-potential therefore has a higher accuracy as well, about ± 20%. It can thus be concluded that water flux measurements at different salt concentrations are a simple method to obtain realistic zeta-potential values.

The effect of charge on the electroviscous effect for a polysulfone membrane is seen in Fig. 2. When increasing the ion concentration (increasing κ), the relative apparent permeability increased and reached a maximum, equalling in this case 1.057. No specific ion adsorption of Na^+ or Mg^{2+} on polysulfone could be detected since there was no difference in permeability increase between monovalent sodium or bivalent magnesium ions, when the difference in charges was compensated for according to Eq. (3).

Fig. 3 shows the variations of the membrane hydraulic resistance (R_m) as a function of the mean TMP for increasing and decreasing TMP and for new and used membranes. Hereafter we use the term "used" membrane for a piece of membrane that has been compressed at least once.

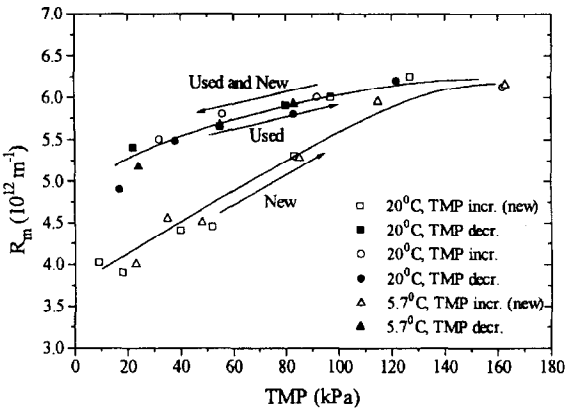

Fig. 3. Membrane resistance vs. TMP for new and used polysulfone capillary membranes at 20 °C and at 5.7 °C. Open symbols are measured while increasing the TMP; closed symbols are measured while decreasing the TMP. Upon increasing the TMP the new membranes and the used membranes follow different trends, but upon decreasing the TMP both used and new membranes follow the same trend.

The solvent used was desalted water at 20 °C and at 5.7 °C, and the membranes used were polysulfone capillary X-Flow membranes.

The resistance R_m increases slightly with TMP. Some hysteresis is observed between a new and a used membrane. When the TMP is increased, the new membrane is compressed for the first time. This compression involves both reversible and irreversible deformation. Therefore there is both a reversible and an irreversible increase in R_m. The compression phenomenon does not depend on temperature in the range 5 to 20 °C.

Fig. 4 shows the variation of R_m as a function of TMP for different solvents (water and water-glycerol mixtures) for X-Flow capillary membranes. All results have been obtained with used membranes. Neither the viscosity nor the temperature have any influence on R_m in this temperature interval, in accordance with expectations, since polymers should be stable below their glass transition temperature. The modest scattering in membrane resistance which is still seen is due to the experimental errors and, of course, the variation in the membrane

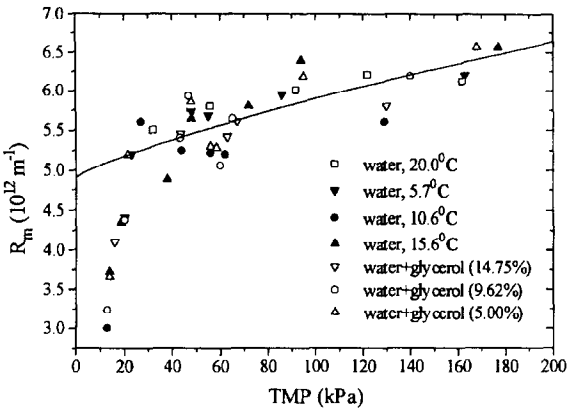

Fig. 4. Membrane resistance vs. TMP for capillary X-flow membranes at various viscosities: □, 1.002 Pa·s; Δ, 1.120 Pa·s; ○, 1.284 Pa·s; ▽, 1.486 Pa·s. Filled symbols represent equal viscosities as open symbols. The solid line represents a curve fit of Eq. (6) assuming n = 0.8.

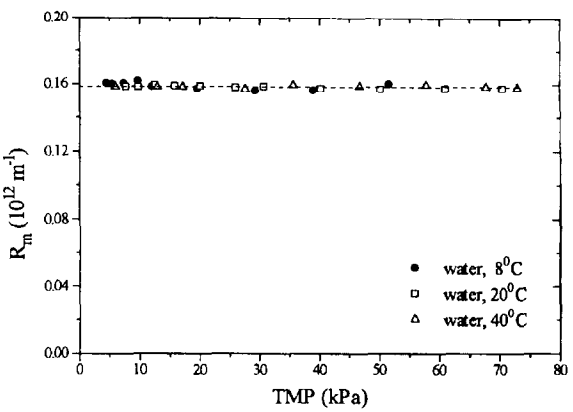

Fig. 5. Membrane resistance vs. TMP for an α-alumina microfiltration membrane at various temperatures.

characteristics between different pieces within a production batch. Thus Darcy's law describes correctly the flow of solvent through the capillary UF membranes if the variation of viscosity is taken into account.

The increase of R_m with TMP shows two regimes: a sharp increase from 0 to 20 kPa, which is partly due to the large errors in both flux and TMP measurements in this interval, and then a slower decrease up to 200 kPa. The solid line in Fig. 4 represents the result of a curve fit of Eq. (6), assuming that the compressibility factor n has the value 0.8 [12]. Only datapoints with TMP above 20 kPa have been taken into account. It is seen that the line describes the increase in membrane resistance very well. It must, however, be mentioned that equally good fits are obtained for all values of n within the interval $0.6 < n < 1$.

Flux measurements were done for the α-alumina membrane at 8°C, 20°C, and 40°C for 0.1 M salt solutions. Results are given in Fig. 5, as membrane resistance vs. TMP. It is clearly seen that no compression occurs and that the membrane resistance does not depend on temperature in the interval 8°C to 40°C. This is in accordance with expectations since ceramics are not expected to be compressible or temperature dependent.

The membrane permeability was found to be independent of temperature, both for the polymeric UF membranes and for the ceramic MF membrane. Other authors have reported increasing membrane permeabilities with increasing temperature [4]. These results may be influenced by the degree of air presolved in the feed solution, which decreases with temperature. Less air in the water means higher measured flux values. The amount of air solved in water can be substantial, especially if the water is RO-treated and has experienced high pressures.

4. Conclusions

For both ceramic MF membranes and polymeric UF membranes, Darcy's law provides an excellent way to describe water permeabilities: electroviscous effects, temperature effects, membrane compressibility, and the effect of the feed viscosity can be taken into account. The polymeric UF membranes used were slightly compressible, which might be a consequence of their high porosity and the visco-elastic nature of polymers. The ceramic MF membrane was not compressible because of the rigid nature of ceramics. The membrane resistance for both MF

and UF membranes was found not to be influenced by temperature.

Electroviscous effects can be utilized in the characterization of membranes. If the pore size is known, the zeta-potential can be calculated from the relative increase in apparent permeability caused by an increase in salt concentration. Observed zeta-potentials had realistic values, both for the UF and MF membranes.

All UF membranes studied displayed a variation in pure water permeability, indicating a variation in pore size distribution between different pieces from the same membrane.

Acknowledgements

Prof. Petr Dejmek is acknowledged for valuable contributions to the discussion and Hoechst AG and X-Flow for kindly supplying the UF membranes. This work was economically supported by NUTEK (K.M. Persson), the European Union (B. Dutré), and the Swedish Foundation for Membrane Technology (I.H. Huisman).

Symbols

e — electron charge, C
F — parameter in Eq. (2)
G — parameter in Eq. (2)
J — permeate flux, m/s
k — Boltzmann constant, J/K
k_c — compressibility constant, m^{-1} Pa^{-n}
r — pore radius, m
R_m — membrane resistance, m^{-1}
$R_{m,a}$ — apparent membrane resistance, m^{-1}
$R_{m,0}$ — pressure independent part of membrane resistance, m^{-1}
T — temperature, K
TMP — transmembrane pressure, Pa

Greek

β — electrolyte parameter
ε_0 — permittivity of vacuum, $C^2 J^{-1} m^{-1}$
ε_r — relative dielectric constant
μ — viscosity, Pa s
μ_a — apparent viscosity of the solution in a capillary, Pa s
μ_0 — bulk viscosity of the solution, Pa s
κ — Debye constant, m^{-1}
λ — electrolyte conductivity, $\Omega^{-1} m^{-1}$
ζ — Zeta-potential, V

References

[1] V. Gekas, G. Trägårdh and B. Hallström, Ultrafiltration membrane performance fundamentals, ISBN 91-630-2231-1, Lund, Sweden, 1993.
[2] A.G. Fane, C.J.D. Fell and A.G. Waters, J. Membr. Sci., 9 (1981) 245.
[3] C. Rosén and C. Trägårdh, J. Membr. Sci., 85 (1993) 139.
[4] V. Tarnawski and P. Jelen, J. Food Eng., 5 (1986) 75.
[5] D.A. Nield and A. Bejan, Convection in Porous Media, Springer Verlag, New York, 1992.
[6] H. Darcy, Les Fontaines Publiques de la Ville de Dijon, V. Dalmont, Paris, 1856.
[7] S. Levine, J.R. Marriott, G. Neale and N. Epstein, J. Colloid Interface Sci., 52(1) (1975) 136.
[8] T.B. Choe, P. Masse, A. Verdier and M.J. Clifton, J. Membr. Sci., 26 (1986) 17.
[9] P. Heinemann, J.A. Howell and R.A. Bryan, Desalination, 68 (1988) 243.
[10] M.D. Moosemiller, C.G.J. Hill and M.A. Anderson, Sep. Sci. Technol., 24 (1989) 641.
[11] F.F. Nazzal and M.R. Wiesner, J. Membr. Sci., 93 (1994) 91.
[12] K.M. Persson, V. Gekas and G. Trägårdh, J. Membr. Sci., 100 (1995) 155.
[13] G. Trägårdh and K. Ölund, Desalination, 58 (1986) 187.
[14] I.H. Huisman, D. Johansson, G. Trägårdh and C. Trägårdh, Trans. ICHemE., 75(A5) (1997) 508.
[15] K.M. Persson, V. Gekas and G. Trägårdh, J. Membr. Sci., 93 (1994) 105.
[16] J.N. Israelachvili, Intermolecular and Surface Forces, Academic Press, London, 1985.
[17] D. Elzo and V. Gekas, Proc., Euromembrane 95, Bath, England, 1995, pp. I-152–156.
[18] M. Nyström, M. Lindström and E. Matthiasson, Coll. Surfaces, 36 (1989) 297.
[19] K.J. Kim, A.G. Fane, M. Nyström, A. Pihlajamäki, W.R. Bowen and H. Mukhtar, J. Membr. Sci., 116 (1996) 149.
[20] J. Nilsson, A study of ultrafiltration fouling, Ph.D. Thesis, Lund University, Sweden, 1989.
[21] I.H. Huisman, G. Trägårdh, A. Pihlajamäki and M. Nyström, Determining the zeta-potential of ceramic microfiltration membranes and its influence on the critical flux for particle suspensions. Presented at NAMS'97, Baltimore, MD, 1997.